STUDY ON CONCEPTS FOR RADAR INTERFEROMETRY FROM SATELLITES FOR OCEAN (AND LAND) APPLICATIONS

Studie zu Konzepten für Radar-Interferometrie über Ozeanen (und Land) im Rahmen zukünftiger Satellitenmissionen

(KoRIOLiS)

SECTION 6: CONCEPT STUDIES

Roland Romeiser, Johannes Schulz-Stellenfleth, and Marcus Schwäbisch

In the previous sections we have discussed the theoretical and technical fundamentals and requirements of current and wave measurements by spaceborne interferometric SAR. We will now evaluate the actual measuring capabilities of several concepts of spaceborne InSAR systems, which have recently been developed and proposed by various authors for various purposes, usually including oceanic measurements as a secondary mission objective.

6.1. EVALUATION METHOD

Noise levels and the accuracy of phase difference measurements by several InSAR configurations have already been calculated in section 5 and elsewhere in the literature. To get an impression of the meaning of the noise figures in terms of the detectability of surface current features (and surface waves), we have generated a model current field and simulated the imaging of these phenomena by several realistic InSAR configurations of interest.

6.1.1. Test Current Field

The test current field is shown in Figure 6-1. It is a two-dimensional current field with an ambient current of 0.5 m/s into the negative y direction and 46 isolated, square-shaped areas of different current gradients and different spatial extension. The size of the squares ranges from 150 m $\times$ 150 m to 1200 m $\times$ 1200 m, and the current gradients range from 0.0001 s^{-1} to 0.0016 s^{-1}, which is a realistic range for weak to moderate current gradients in coastal areas. The grid resolution is 25 m $\times$ 25 m. Spatially varying wave spectra over this current field were computed by the M4S model for wind speeds of 5 m/s and 10 m/s and a wind direction toward the lower right corner of the current field.

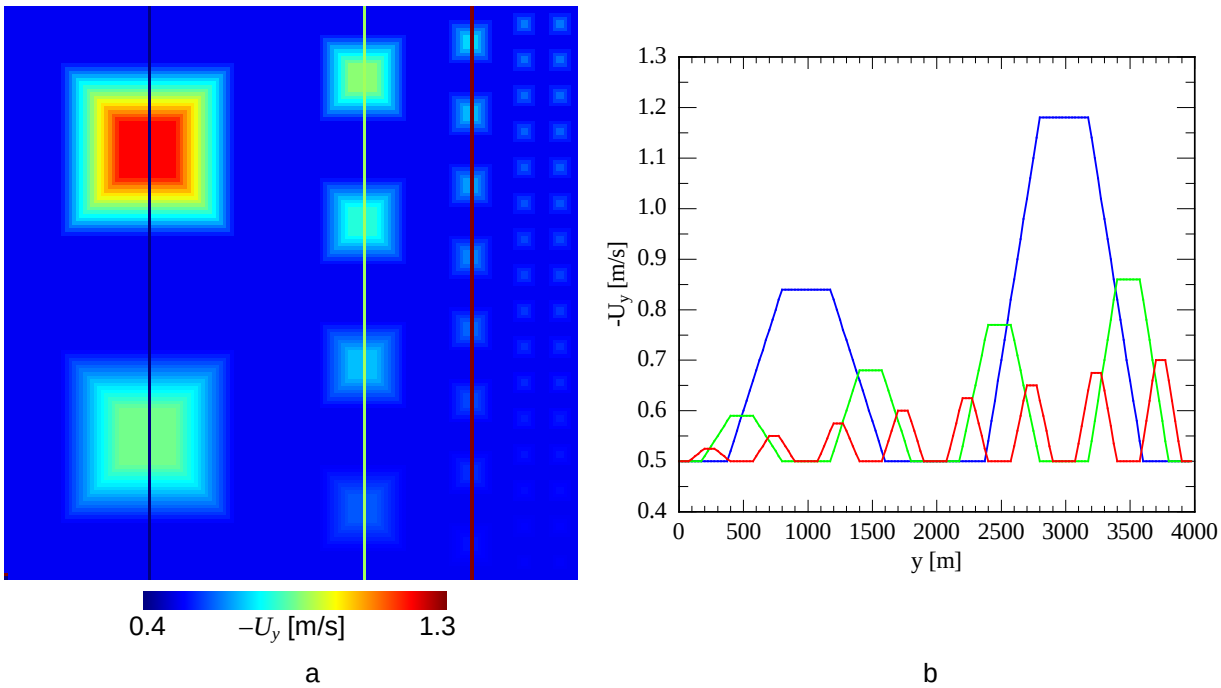

Figure 6-1: Model current field for ATI performance simulations (a) and transects along three columns (b); flow direction is toward the negative y direction (everywhere); grid cell size is 25 m $\times$ 25 m.

6.2. THE "INTERFEROMETRIC CARTWHEEL"

The concept of the "Interferometric Cartwheel" was developed by French scientists [*Massonnet*, 1999; *Massonnet et al.*, 2000; *Ramongassié et al.*, 2000] and has been proposed in various configurations and for various applications. The basic idea is that one would like to have an XTI system in space which always offers a sufficient cross-track antenna separation for topographic mapping or other (land) applications of XTI. For a short time this could be achieved by two satellites flying near each other at different altitudes, but different orbits are associated with different cycle periods, thus it would be impossible to maintain a constant horizontal distance between the satellites.

6.2.1. Concept

The "Interferometric Cartwheel" solves this problem by using three satellites on elliptical orbits, which have the same orbital plane and the same dimensions, thus the same cycle period, but whose main axes are rotated against each other, and the motions are phased in such a way that the satellites form a kind of rotating triangle, as shown in Figure 6-2. This way, there is always a sufficient cross-track separation between at least two satellites. Of course, the satellite at lowest altitude will still pass the higher ones in this arrangement, but in later phases it will arrive at higher altitudes and lower speeds and be passed by the others again. From a frame which moves with the center of gravity of the three satellites, all satellites move along the same elliptical trajectory with one revolution per orbit cycle, forming the "Cartwheel". The ratio between the length and the height of an "Interferometric Cartwheel" is 2 and cannot be tuned.

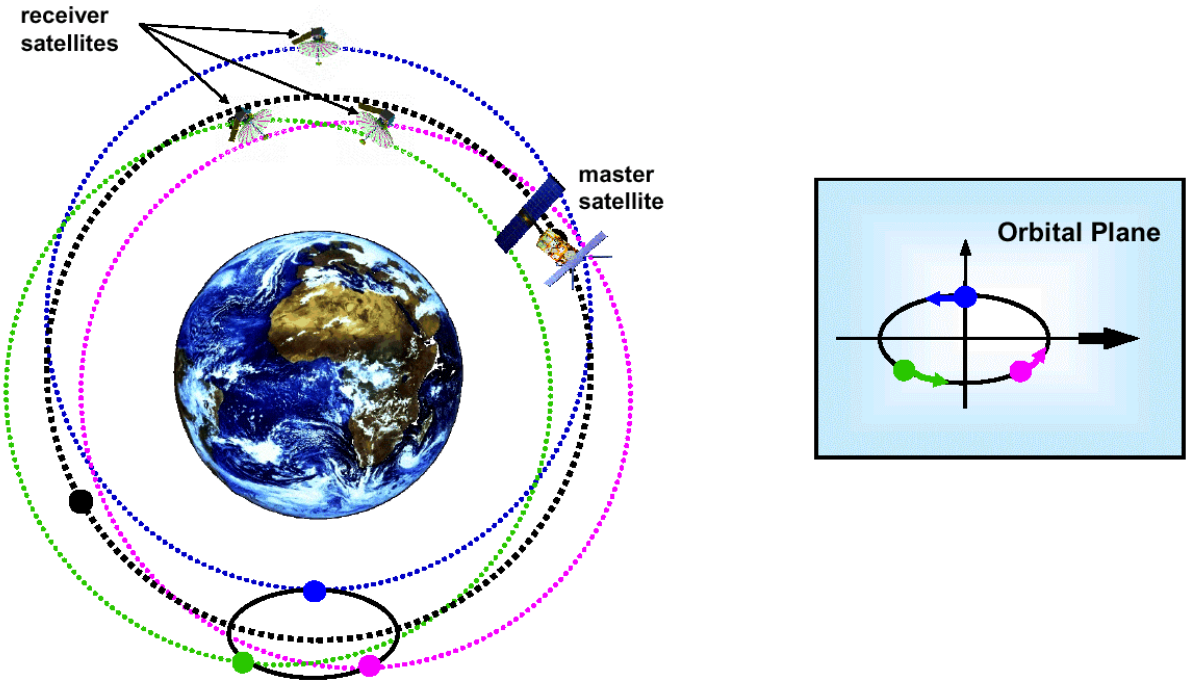

Figure 6-2: Orbit configuration of an "Interferometric Cartwheel" of three microsatellites following a master satellite (figure provided by A. Moreira, German Aerospace Center).

In addition to the three satellites which form the "Interferometric Cartwheel", Figure 6-2 shows a bigger "master satellite", which acts as transmitter of the SAR signals. This is a part of the concept: The "Cartwheel" satellites are cheap microsatellites, which carry only receiving antennas and depend on the signal generated by an existing bigger satellite with a conventional SAR system. For timing reasons, the separation between the "Cartwheel" and the master satellite would usually be on the order of tens of kilometers [*Mittermayer et al.*, 2001a, b], while ideal dimensions of the "Cartwheel" ellipse would be on the order of a few 100 meters to some kilometers, depending on the radar frequency. Usually, only data from the three "Cartwheel" satellites would be used for interferometry – they would not be combined with the monostatic SAR data received by the master satellite itself.

Figure 6-3 shows details of the orbit geometry and the resulting effective XTI baselines of an "Interferometric Cartwheel". For ocean applications, not this XTI baseline, but the along-track antenna separation and the corresponding ATI time lag are the most important parameters, since they determine the coherence of the backscattered signal and the sensitivity of the InSAR to velocity variations. We analyze the potential of three "Cartwheel" configurations which have been discussed in recent publications and proposals: A "Cartwheel" behind the European satellite *ENVISAT* with a multi-polarization C-band SAR [*Runge et al.*, 2001; *Mittermayer et al.*, 2001a, b] and "Cartwheels" behind *TerraSAR* with an X-band SAR or an L-band SAR, as already considered in section 5. The system parameters of the three systems are summarized in Table 6-1.

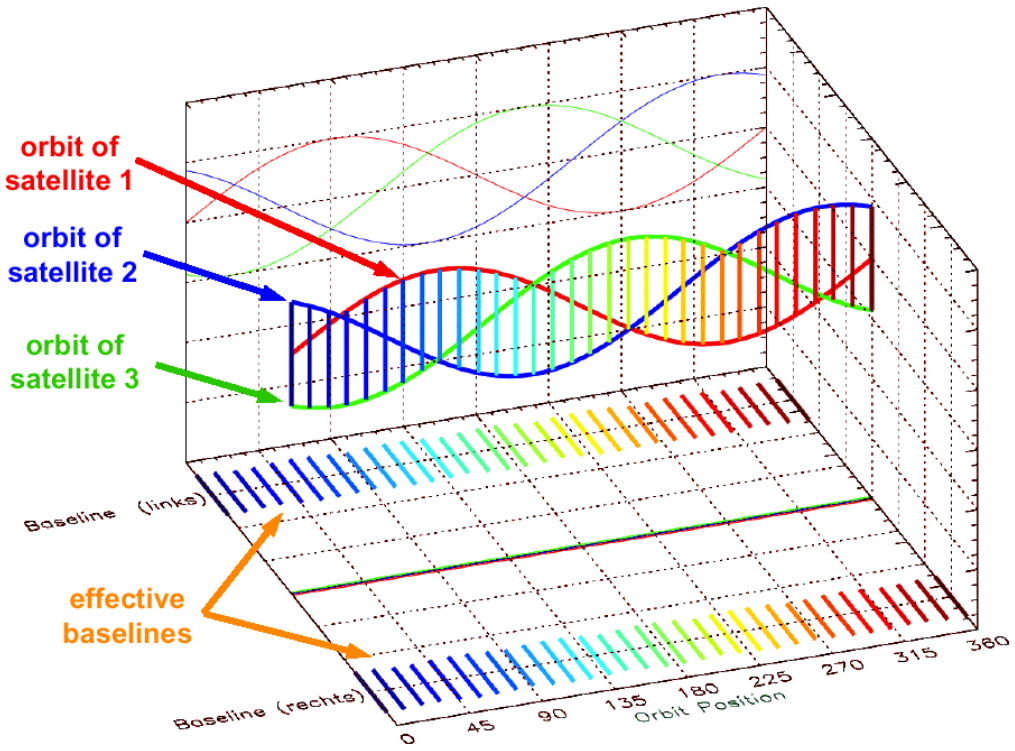

Figure 6-3: Variation of the flight altitudes of the three "Cartwheel" satellites as functions of the orbital phase and resulting effective XTI baselines (figure provided by A. Moreira, German Aerospace Center).

Table 6-1: System parameters of three potential "Interferometric Cartwheel" configurations.

Master Satellite	*ENVISAT*[1]	*TerraSAR-X*	*TerraSAR-L*
Radar Frequency [GHz]	5.3	9.7	1.5
Polarization	VV	VV	VV
Incidence Angle [deg]	43	33.8	33.8
Altitude [km]	800	514	514
Velocity [m/s]	7000	7000	7000
Eff. No. of Looks[2]	5.6	230	20
Noise Equ. NRCS [dB]	–18.0	–27.9	–36.3

[1]) Proposed special "Interferometric Cartwheel" mode of ASAR
[2]) Effective number of looks for a 25 m × 25 m resolution cell

6.2.2. Simulated Data Products

Figure 6-4 shows simulated expectation value phase images of the test current field at a wind speed of 5 m/s, as seen by the three "Interferometric Cartwheel" configurations. These expectation value results correspond to averages over an infinite number of samples, that is, they do not exhibit any signatures of statistical fluctuations. Since the InSAR time lags are very short in this example, the absolute phase differences are not very large, but a coherence of almost 1 is obtained. Nevertheless, a comparison of these phase signatures with the original current field as shown in Figure 6-1 reveals clear nonlinearities in the imaging mechanism, which result from the modulation of surface waves by the spatially varying currents and from the fact that the wind direction is 45° off the current flow direction. The most linear imaging of the current variations is obtained for the *ENVISAT* "Cartwheel" (Figure 6-4a), which is a result of its high incidence angle of 43°. For the steep incidence angle of *TerraSAR* (33.8°), the InSAR imaging is found to be more linear at L-band (Figure 6-4c) than at X-band (Figure 6-4b). The same behavior but even more pronounced nonlinearities are found for a wind speed of 10 m/s (Figure 6-5). Note that the small current features near the lower right corner of the test current field are not discernible anymore under these conditions, even with a perfect, noise-free InSAR system. Aside from such "hard" limitations, most of the nonlinearities of the InSAR imaging mechanism can be corrected by the iterative current field retrieval procedure presented in section 3.

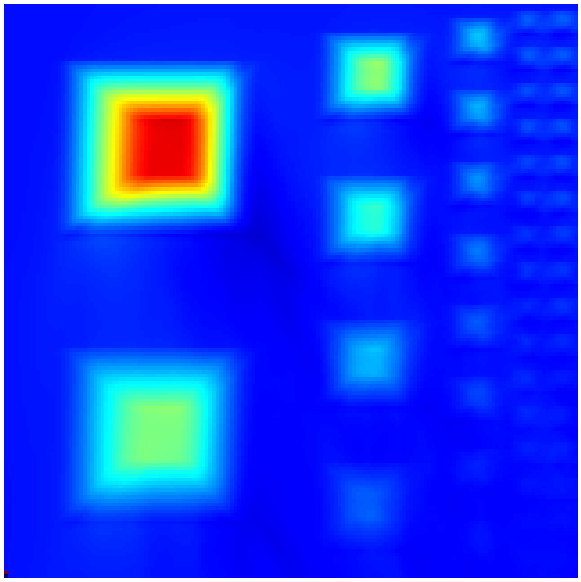

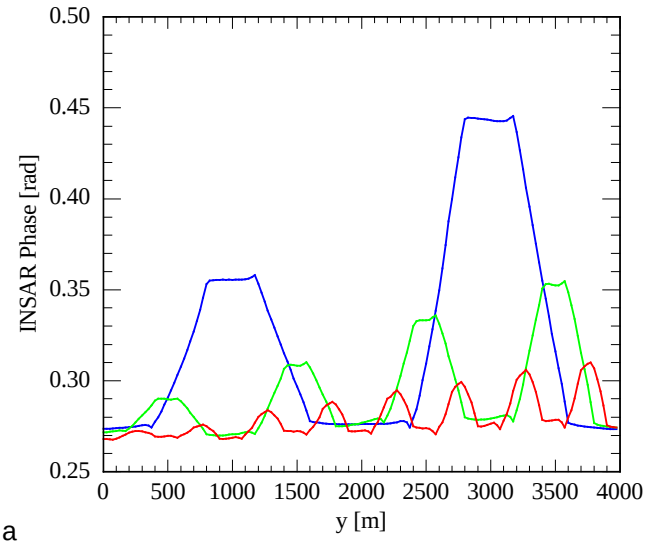

a

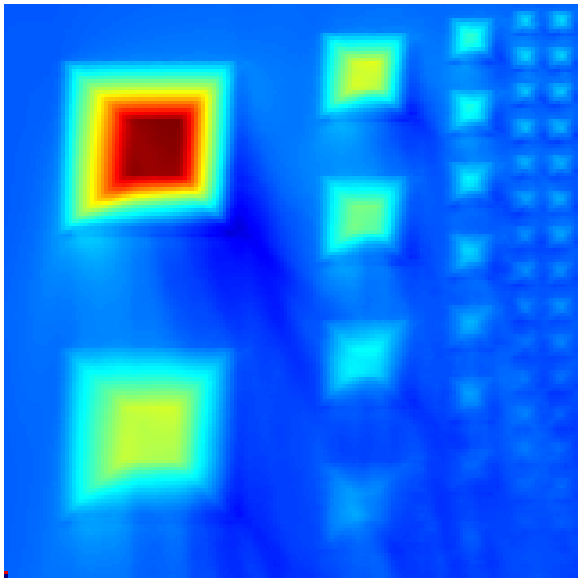

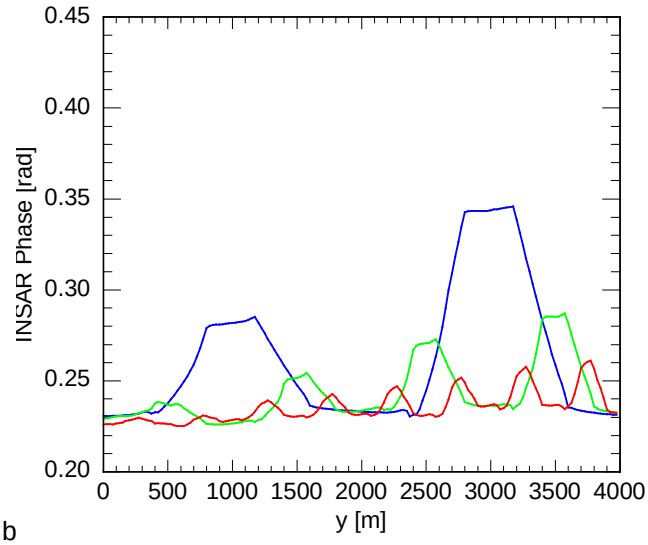

b

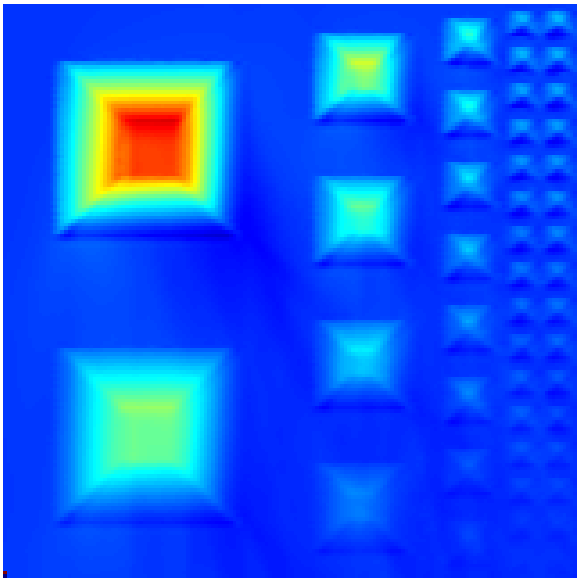

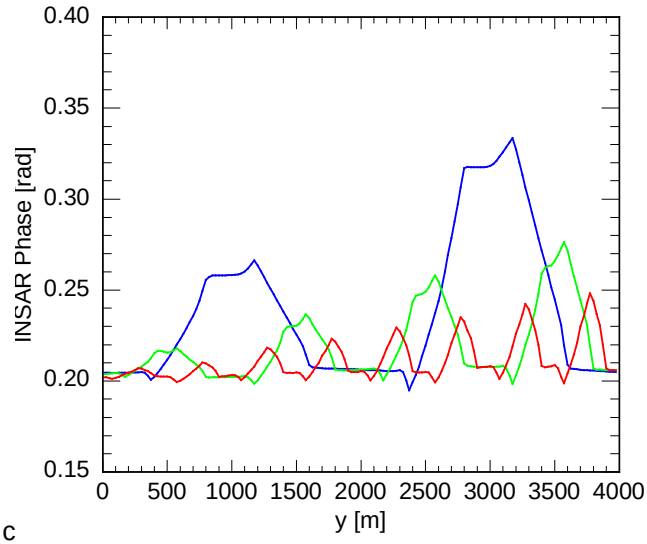

c

Figure 6-4: Simulated expectation value InSAR phase signatures of the current field of Figure 6-1 for spaceborne "Interferometric Cartwheels" behind (a) ENVISAT ($\tau = 2$ ms, $\rho = 0.99$), (b), TerraSAR-X ($\tau = 1$ ms, $\rho = 0.99$), (c) TerraSAR-L ($\tau = 6$ ms, $\rho = 0.99$); look direction: from bottom to top (i.e. against the current); flight direction: from left to right; wind: 5 m/s toward lower right corner; colorcoding (left column) and scaling of vertical axes (right column) have been individually adjusted for best visibility of signatures.

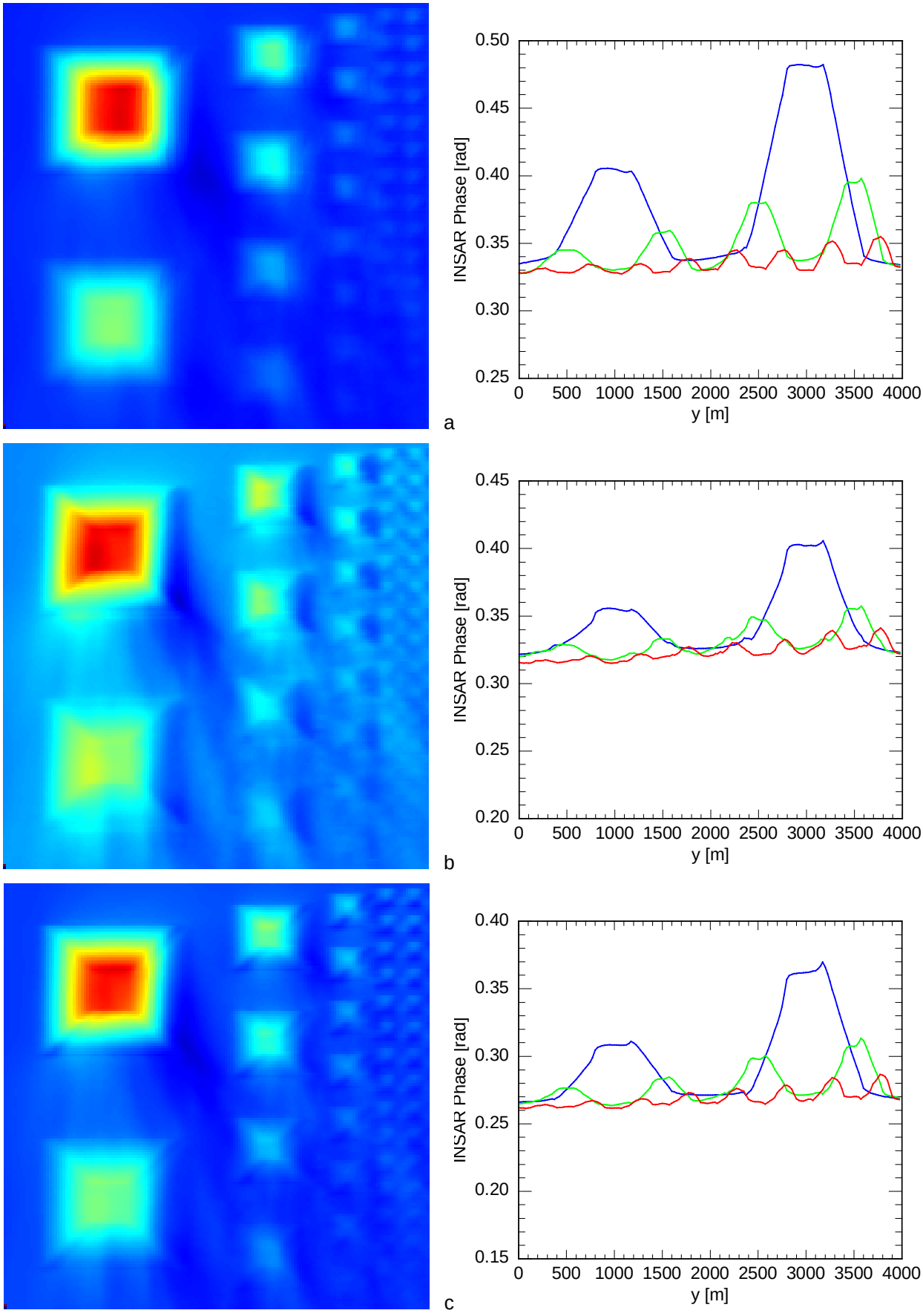

Figure 6-5: Same as Figure 6-4, but for a wind speed of 10 m/s; ρ = 0.97.

Let us now consider simulated realizations of actual phase images, as they would be obtained from the InSAR systems in a real experiment. Such data include phase noise as a result of the limited coherence of the signal, instrument noise, and a limited number of independent samples (looks) per resolution cell. Figure 6-6 shows simulation results for the *ENVISAT* "Cartwheel" at a wind speed of 5 m/s. The phase images are clearly dominated by noise; only the two most pronounced features on the left-hand side of the test current field are faintly visible for time lags between about 8 and 30 ms. A comparison with Figure 6-7, which shows simulation results for the same scenario without instrument noise, reveals that the main problem of the *ENVISAT* "Cartwheel" is its high instrument noise, which dominates the relatively low backscatter from the sea surface at an incidence angle of 43° and a wind speed of 5 m/s. Other ASAR modes with steeper incidence angles may be better suited for interferometry over water.

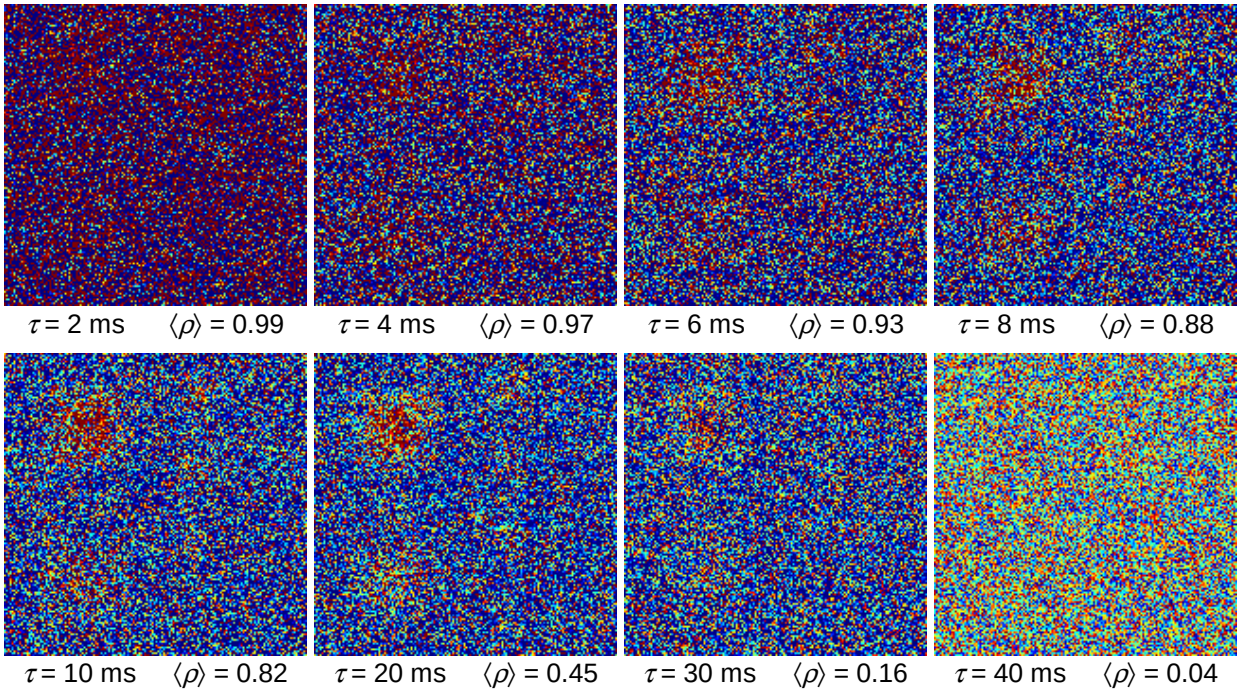

Figure 6-6: Simulated realizations of phase images of the current field of Figure 6-1 as seen by the proposed "Interferometric Cartwheel" behind ENVISAT for different time lags τ and corresponding mean coherences $\langle\rho\rangle$ of the backscattered signal; wind: 5 m/s toward lower right corner; colorcoding has been individually adjusted for best visibility of the signatures.

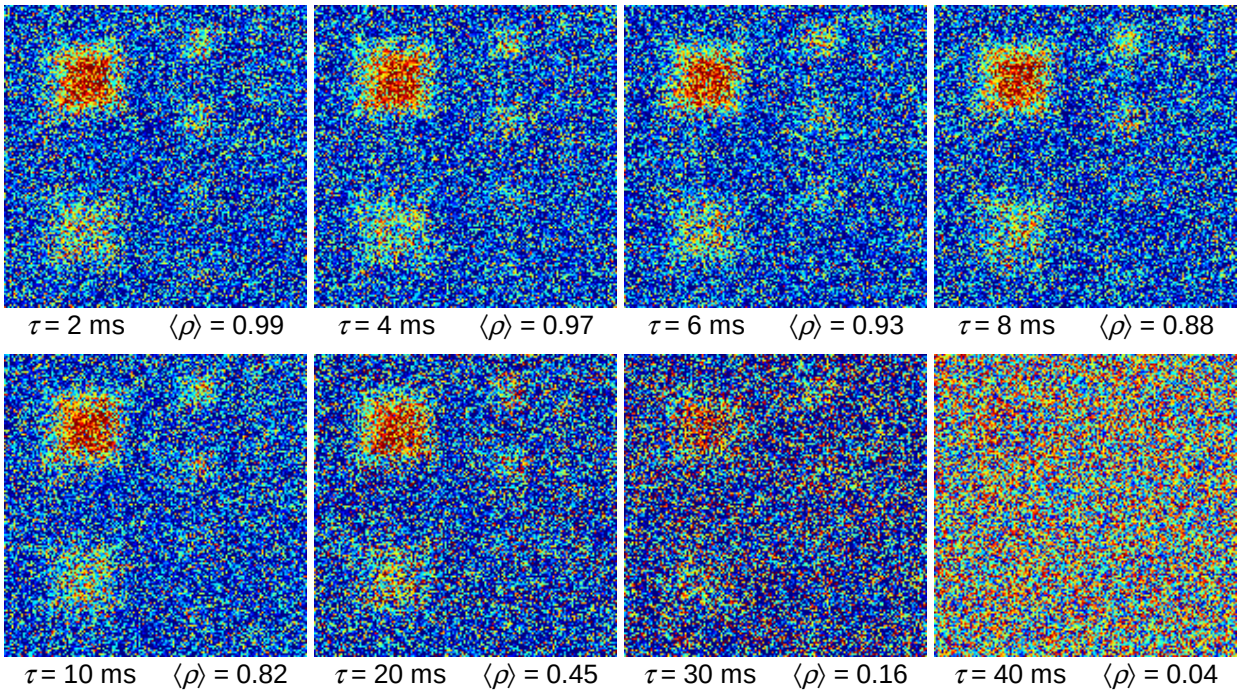

Figure 6-7: Same as Figure 6-6, but without instrument noise.

Figure 6-8 shows *ENVISAT* "Cartwheel" simulation results for a wind speed of 10 m/s. Although the normalized radar backscattering cross section (NRCS) of the sea surface, and thus the signal-to-noise ratio (SNR), should be significantly better at this wind speed, the phase noise is even worse than in the 5 m/s case. Figure 6-9 shows that also the simulation results without instrument noise are quite noisy for 10 m/s winds. In this case the phase noise results from the reduced coherence and from the relative small effective number of looks (5.6) of the *ENVISAT* "Cartwheel", which does not lead to a sufficient noise reduction. A reduction of the spatial resolution by further averaging can compensate for this problem.

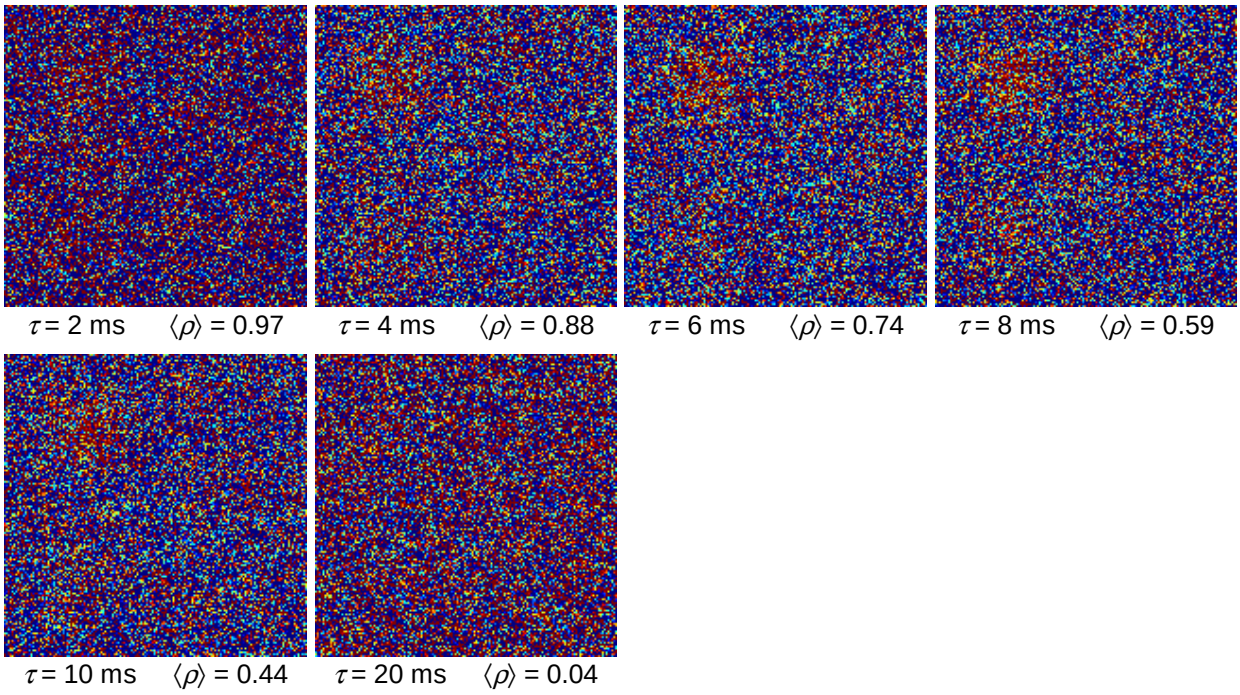

Figure 6-8: Same as Figure 6-6, but for a wind speed of 10 m/s.

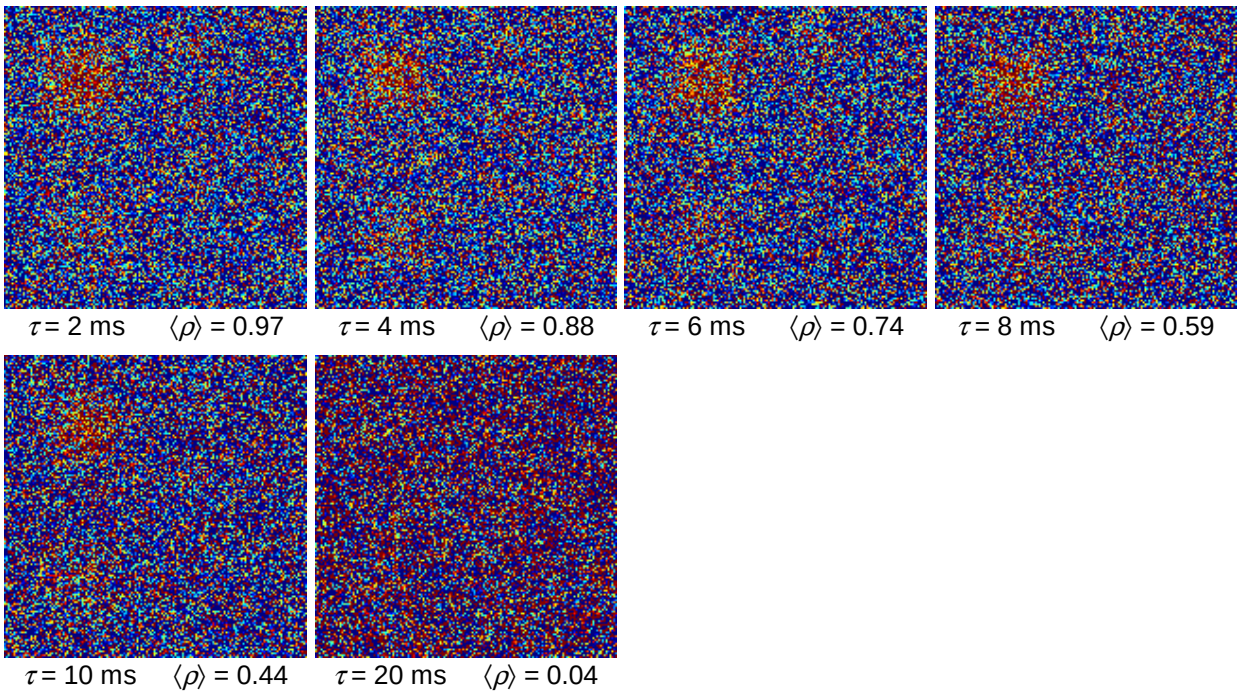

Figure 6-9: Same as Figure 6-8, but without instrument noise.

Figures 6-10 and 6-11 show simulation results for the *TerraSAR-X* "Cartwheel" at wind speeds of 5 m/s and 10 m/s, respectively, including instrument noise. These phase images look much better than the ones from the *ENVISAT* simulations, since the instrument noise level is lower (about 16 dB SNR (single look) instead of 2.3 dB in the *ENVISAT* case, according to the M4S model) and the effective number of looks (230) is larger by a factor of about 40. Time lags between about 1 ms and 20 ms can be used for current measurements at low wind speeds. At 10 m/s winds, the coherence becomes too low for time lags beyond approx. 5 ms. High phase noise is also found for very short time lags below 1 ms, where phase fluctuations resulting from instrument noise dominate the very small phase differences associated with surface currents. Under ideal conditions (low wind speed and time lags between 1 and 10 ms) the *TerraSAR-X* "Cartwheel" should be capable of detecting current variations on the order of 0.1 m/s on length scales on the order of 100 m.

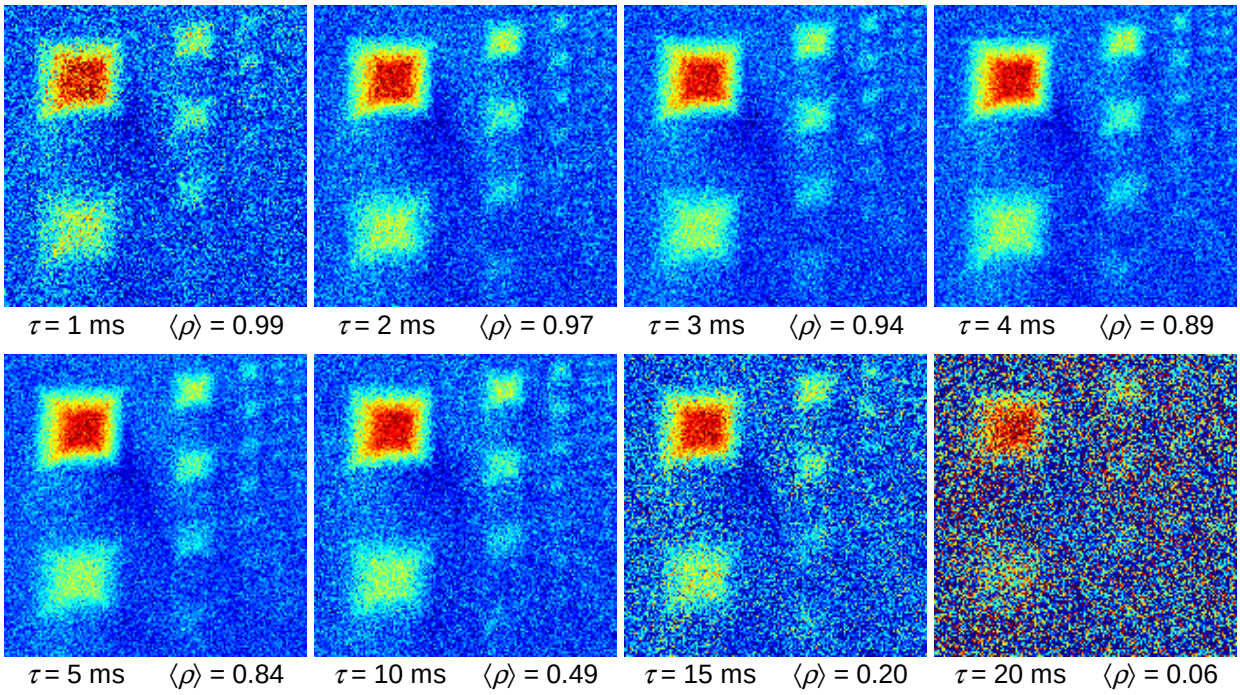

Figure 6-10: Same as Figure 6-6, but for TerraSAR-X parameters instead of ENVISAT parameters.

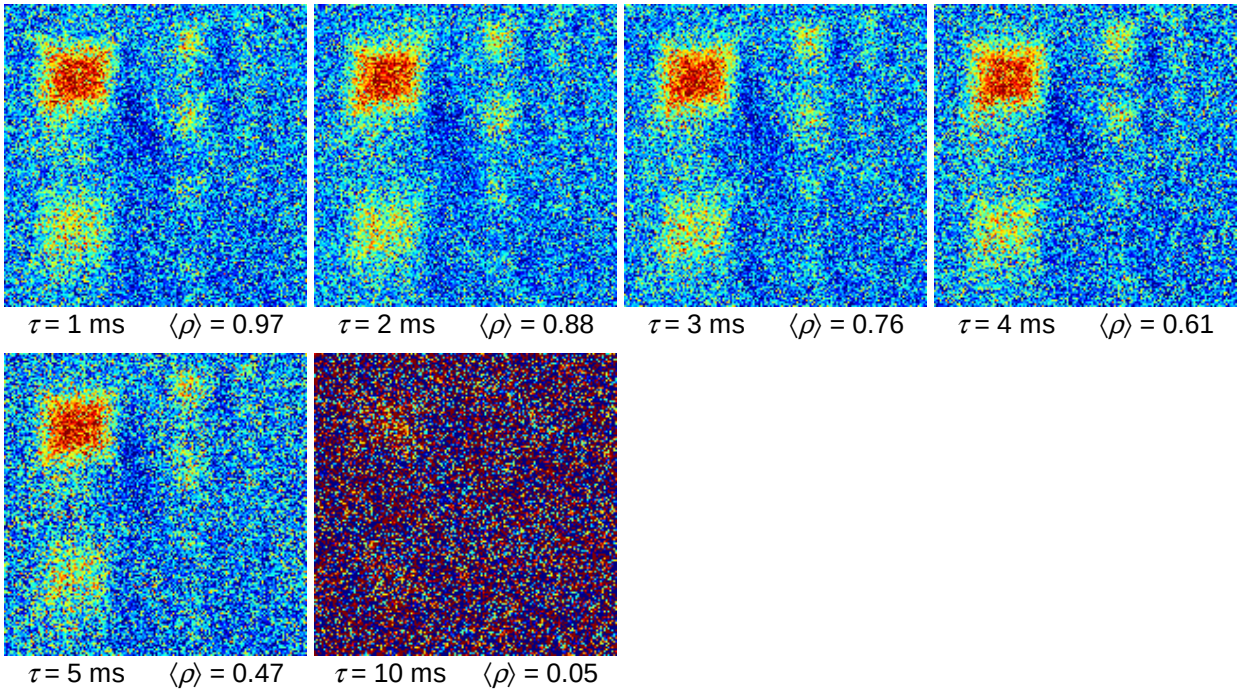

Figure 6-11: Same as Figure 6-10, but for a wind speed of 10 m/s instead of 5 m/s.

Finally, Figures 6-12 and 6-13 show simulation results for the *TerraSAR-L* "Cartwheel". At least for low wind speeds, the detectability of current features is not too bad for time lags up to about 60 ms. Also very short time lags can be used, since the SNR is quite high (about 27 dB at 5 m/s). However, due to the fact that the effective number of looks is smaller than in case of the *TerraSAR-X* "Cartwheel" by a factor of about 11, *TerraSAR-X* is the clear favorite of the three "Interferometric Cartwheel" concepts considered here, as far as oceanic measurements are concerned.

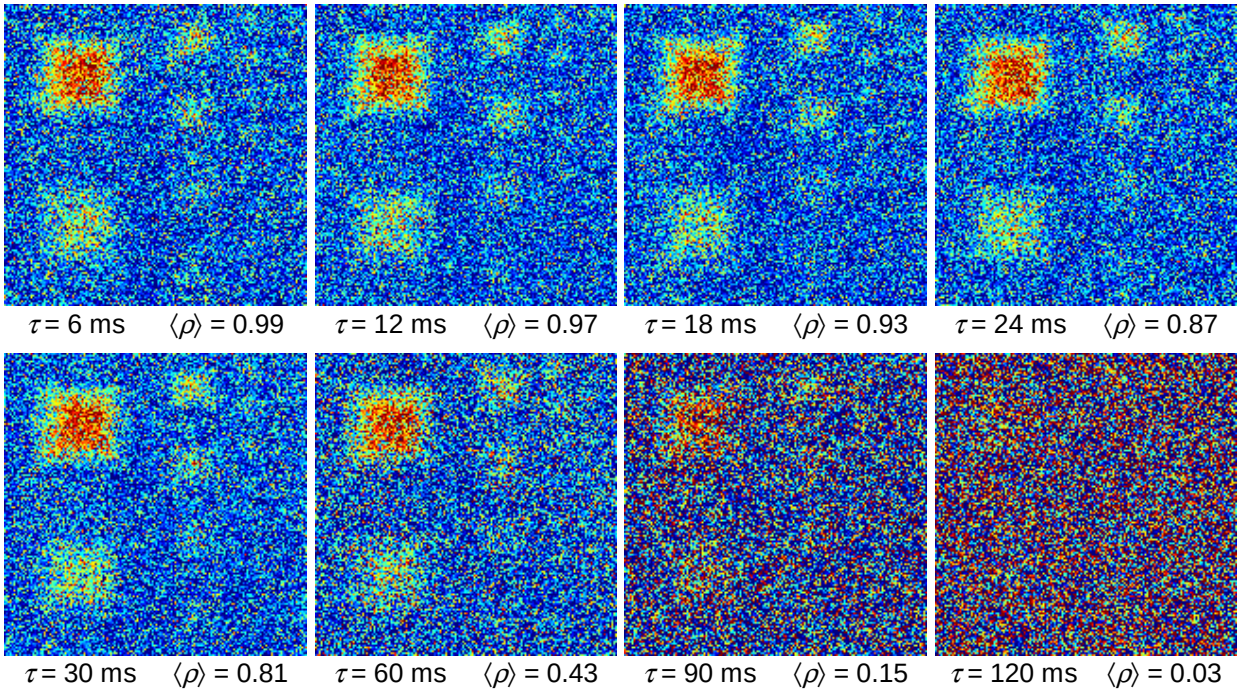

Figure 6-12: Same as Figure 6-6, but for TerraSAR-L parameters instead of ENVISAT parameters.

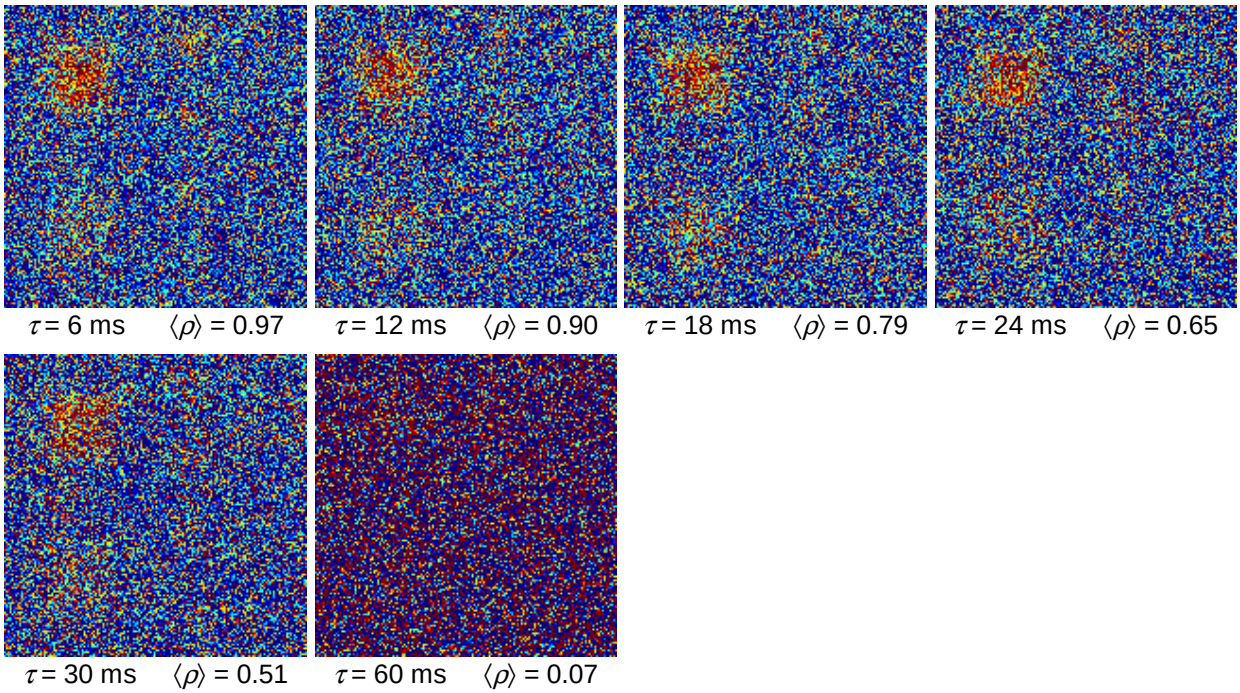

Figure 6-13: Same as Figure 6-12, but for a wind speed of 10 m/s instead of 5 m/s.

6.2.3. Evaluation

Our model results indicate that oceanic measurements by the "Interferometric Cartwheel" could be performed quite well for time lags between about 1 ms and 15 ms at X-band (*TerraSAR-X* "Cartwheel") and for time lags up to about 90 ms at L-band (*TerraSAR-L* "Cartwheel"). The corresponding range of time lags for a C-band system (*ENVISAT* "Cartwheel"), which basically scales with the radar wavelength, would be between about 2 ms and 30 ms, regardless of the fact that the simulation results for the *ENVISAT* "Cartwheel" exhibit hardly any signatures of current variations due to a high instrument noise level and a small effective number of looks. For best XTI performance, the proposed "Cartwheel" with *ENVISAT* has a length of 2500 m and a height of 1250 m [*Mittermayer et al.*, 2001a]. Also these "ideal" dimensions scale with the radar wavelength, thus the following time lag analysis of the *ENVISAT* "Cartwheel" is representative for all "Cartwheel" concepts.

Figure 6-14 shows the available time lags between three pairs of microsatellites of the *ENVISAT* "Cartwheel" as function of the orbit latitude, for ascending and descending orbit segments, and for three different phasing arrangements of the three microsatellites. Hatched areas in the plots indicate the range of time lags which would be suited for interferometry. The figure depicts that sufficiently short time lags for interferometry over water would be obtained in limited areas only, which form three to six belts around the globe with a width of about 20 degrees for each belt. The number and the location of the belts depends on the phasing of the "Cartwheel" satellites: Figure 6-14a shows the timing for an arrangement with one satellite at the highest altitude when the "Cartwheel" reaches the northernmost point of its orbit. In this case, interferometric current and wave measurements can be performed during ascending and descending overflights of three latitudinal bands, including the equator. Also the arrangement shown in Figure 6-14b permits measurements during ascending and descending overflights of the same bands, but in this case two wide bands (width: about 20 degrees) and two narrow bands (about 10 degrees) are obtained, and the equator is not included. Finally, the arrangement of Figure 6-14c leads to different coverages during ascending and descending overflights, thus six bands where current and wave measurements are possible. Since the maximum available cross-track antenna separation of the "Interferometric Cartwheel" is almost constant, the phasing of the three satellites should not matter very much for land applications. It should thus be optimized for best coverage of test areas of interest in the ocean.

We conclude that the "Interferometric Cartwheel" is not perfectly suited for current and wave measurements, but the proposed *TerraSAR-X* configuration in combination with a favorable phasing of the three satellites could be quite attractive for measurements in limited areas of interest, such as the North Sea or, say, the east coast of the U.S. with the Gulf Stream. Also the *TerraSAR-L* "Cartwheel" would be useful for such activities. The proposed *ENVISAT* "Cartwheel" would not be suited for oceanic measurements because its noise level is too high and its spatial resolution is too coarse.

Aside from these findings on current and wave measurements, one should be aware of the fact that, in addition to current and wave measurements, a "Carthweel" would also be suited for the detection of sea ice (on the basis of coherence differences), for ice thickness measurements (by cross-track interferometry), ice type classification (using polarimetric signatures) and ice drift velocity measurements. Since ice drift velocities are usually smaller than ocean currents and the coherence of the radar backscatter from ice is much higher than the coherence of signals from open water, one could use relatively long time lags for ice drift observations, thus a "sea ice mission" with an "Interferometric Cartwheel" would not suffer from the time lag constraints which limit the measuring capabilities over water.

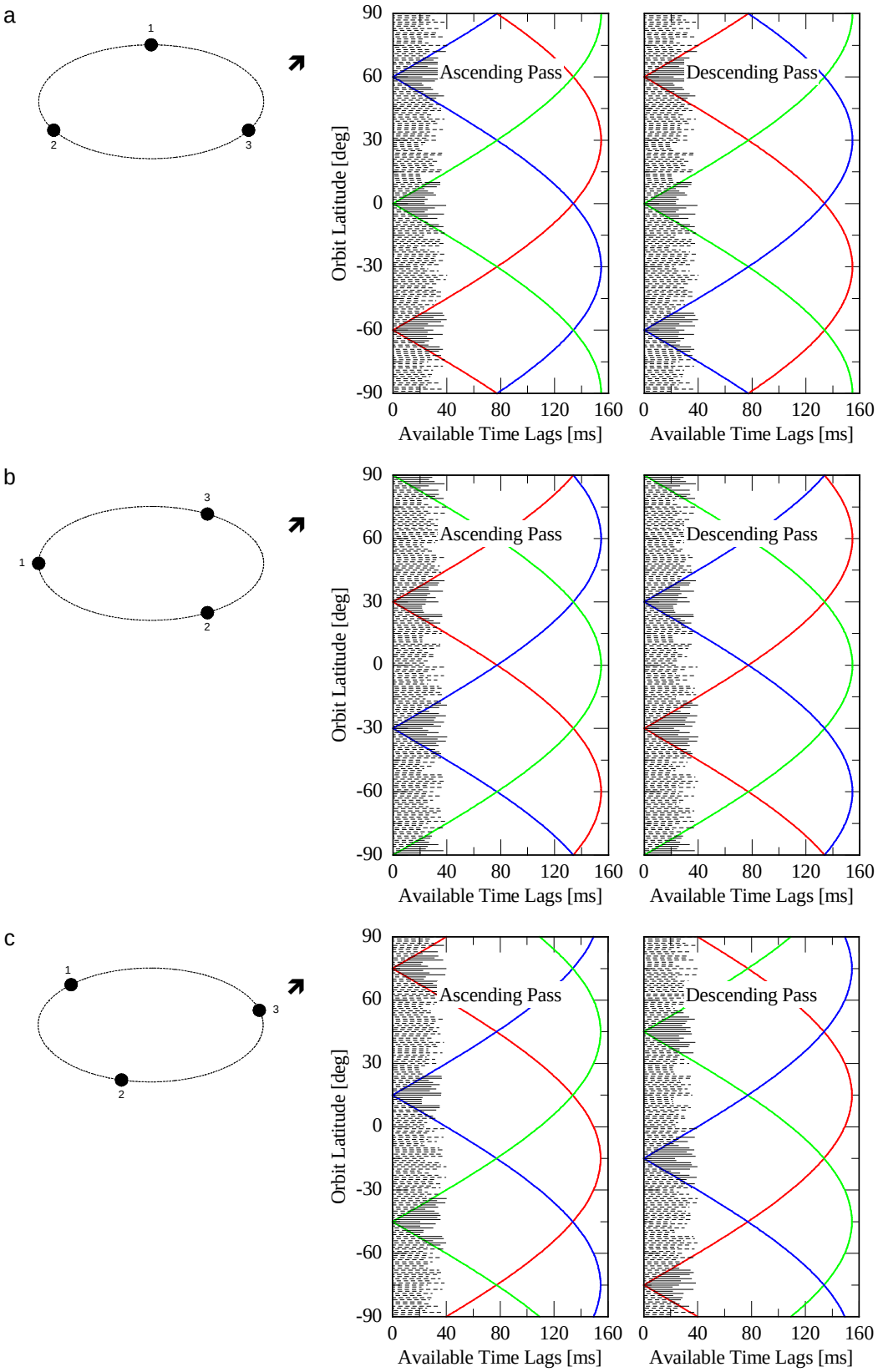

Figure 6-14: Available time lags between three pairs of satellites of the proposed "Interferometric Cart-wheel" behind ENVISAT as function of orbit latitude, for different phasing arrangements: (a) one satellite at maximum altitude at northernmost point of orbit, (b) one satellite at mean altitude at northernmost point, (c) intermediate setting; hatched areas indicate reasonable coherence.

6.3. THE "INTERFEROMETRIC PENDULUM"

The concept of the "Interferometric Pendulum" was proposed by Alberto Moreira and co-workers at the German Aerospace Center as a result of their investigations on the "Interferometric Cartwheel". The two concepts are very similar, but the "Interferometric Pendulum" has appealing advantages, which could be particularly useful for ocean applications.

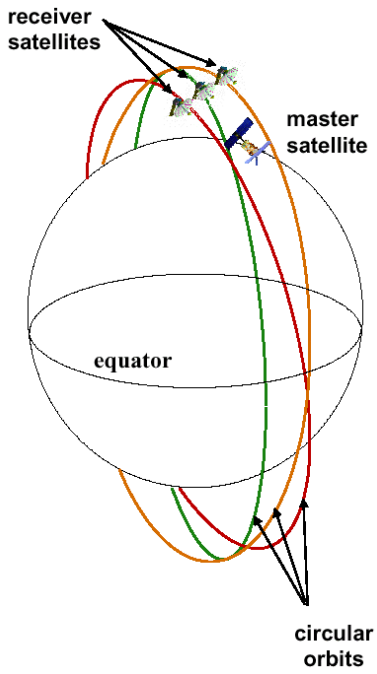

Figure 6-15: Orbit configuration of an "Interferometric Pendulum" of three microsatellites following a master satellite (figure provided by A. Moreira, German Aerospace Center).

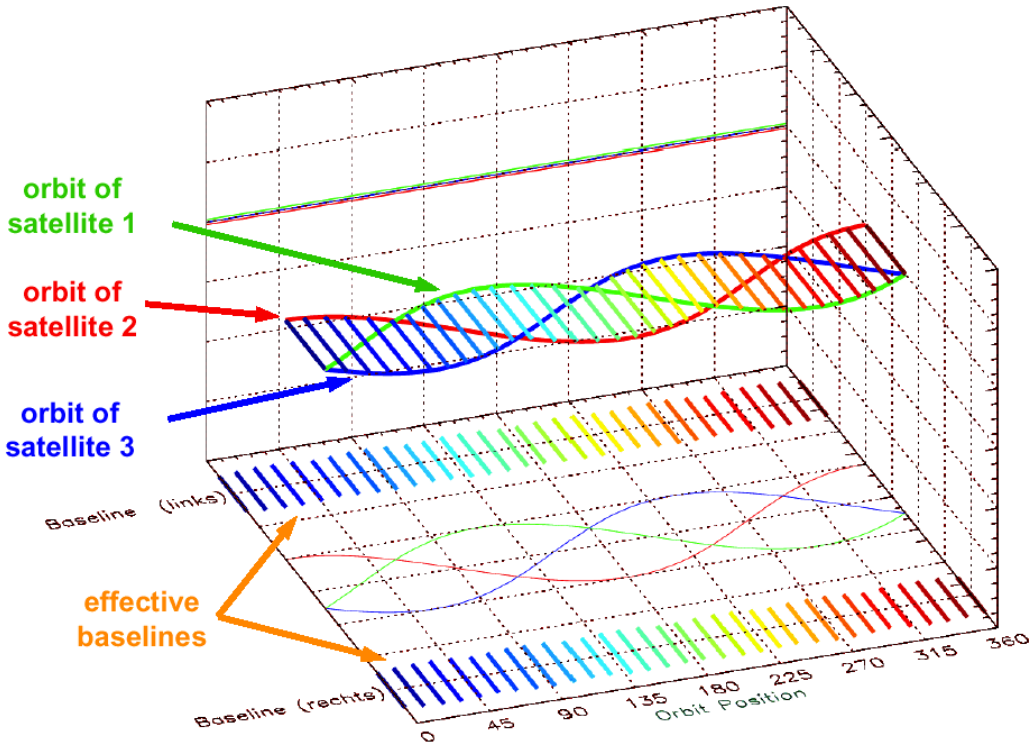

Figure 6-16: Effective lateral positions of the three "Pendulum" satellites as functions of the orbital phase and resulting effective XTI baselines (figure provided by A. Moreira, German Aerospace Center).

6.3.1. Concept

While the three microsatellites of an "Interferometric Cartwheel" are on elliptical orbits in a common orbital plane and form cross-track InSAR baselines in the vertical direction, the "Interferometric Pendulum" uses three satellites on circular orbits with slightly different ascending nodes and inclinations, as shown in Figures 6-15 and 6-16. In this case, cross-track baselines are formed in the horizontal direction. The along-track distances between the satellites are constant and completely independent of the cross-track baselines. That is, the along-track baselines can be freely adjusted to obtain best performance for oceanic measurements.

6.3.2. Simulated Data Products

Since the hardware components of the "Interferometric Pendulum" do not differ from those of the "Interferometric Cartwheel", the simulation results of 6.2.2 are also valid for the "Pendulum". The main difference between "Cartwheel" and "Pendulum" with respect to ocean applications is the fact that the along-track distances between the satellites of the "Pendulum" are freely selectable. Instead of discussing the achievable coverage of different latitudinal regions by current and wave measurements, the evaluation can focus on the selection of antenna distances / time lags which promise best possible performance for current and wave measurements.

6.3.3. Evaluation

We propose to select different along-track distances between the first and the second and between the second and the third satellite of the "Interferometric Pendulum" in order to obtain three different time lags for measurements with different coherences and different sensitivities. The shortest time lag should be long enough to ensure sufficient sensitivity to current variations and to avoid collisions of the satellites at orbit crossings. The longest time lag should be short enough to ensure sufficient coherence, at least for low wind speeds, but long enough for a high sensitivity to current variations, which may be very useful, for example, for measurements of small currents with high accuracy and for sea ice velocity measurements. The proposed distances and corresponding time lags, coherences, and horizontal velocity ranges mapped into a 2π interval are summarized in Table 6-2. "Interferometric Pendulum" configurations with the proposed time lags would be clearly superior to any "Interferometric Cartwheel", because they could be used for current and wave measurements with constant quality at any place and at any time.

Table 6-2: Proposed along-track distances and corresponding time lags, coherences, and horizontal velocity ranges mapped into a 2π interval, for three possible "Interferometric Pendulum" configurations (for technical parameters of the configurations see Table 6-1).

Master Satellite	*ENVISAT*	*TerraSAR-X*	*TerraSAR-L*
Spacing Sat-1 – Sat-2 [m]	140	70	420
Corresponding Time Lag [ms]	10	5	30
Coherence (Wind = 5 m/s)	0.82	0.83	0.81
Coherence (Wind = 10 m/s)	0.44	0.45	0.50
Velocity Range (2π) [m/s]	4.15	5.56	5.99
Spacing Sat-2 – Sat-3 [m]	280	140	840
Corresponding Time Lag [ms]	20	10	60
Coherence (Wind = 5 m/s)	0.45	0.48	0.44
Coherence (Wind = 10 m/s)	0.04	0.04	0.07
Velocity Range (2π) [m/s]	2.07	2.78	3.00
Spacing Sat-1 – Sat-3 [m]	420	210	1260
Corresponding Time Lag [ms]	30	15	90
Coherence (Wind = 5 m/s)	0.16	0.19	0.16
Coherence (Wind = 10 m/s)	–	–	–
Velocity Range (2π) [m/s]	1.38	1.85	2.00

6.4. INSAR ON THE *INTERNATIONAL SPACE STATION*

The *International Space Station* (*ISS*) could be an attractive platform for an interferometric SAR, since it is an existing structure in space with sufficient dimensions to accomodate both InSAR antennas and with sufficient power supply and data downlink capacities. A detailed analysis of all aspects of an InSAR on the *ISS* would be beyond the scope of this study, but we discuss some key issues and present example data products.

6.4.1. Concept

The layout of the *ISS* is shown in Figure 6-17. Furthermore, Table 6-3 summarizes some key parameters. The main fuselage has a length of about 74 m. We assume that two antennas in an along-track InSAR configuration could be installed with a distance of about 40 m, which corresponds to an InSAR time lag of 5 ms if both antennas are transmitting and receiving and 2.5 ms if only one antenna acts as transmitter. Since S-band and K_u-band are used for communications, these frequency bands should be avoided by the SAR. We assume that an X-band InSAR system is used, whose parameters and noise figures are very similar to those of the *TerraSAR-X* system, except for a larger incidence angle of 40°, which is better suited for oceanic measurements than the incidence angle of *TerraSAR* of 33.8°. The system parameters of the proposed InSAR system are summarized in Table 6-4. Figure 6-18 shows the ground track pattern of the *ISS*, which results from its orbit altitude of about 400 km and the inclination of 51.6°. Oceanic regions between approx. 51.6°S and 51.6°N could be covered by current and wave measurements with an InSAR system on the *ISS*.

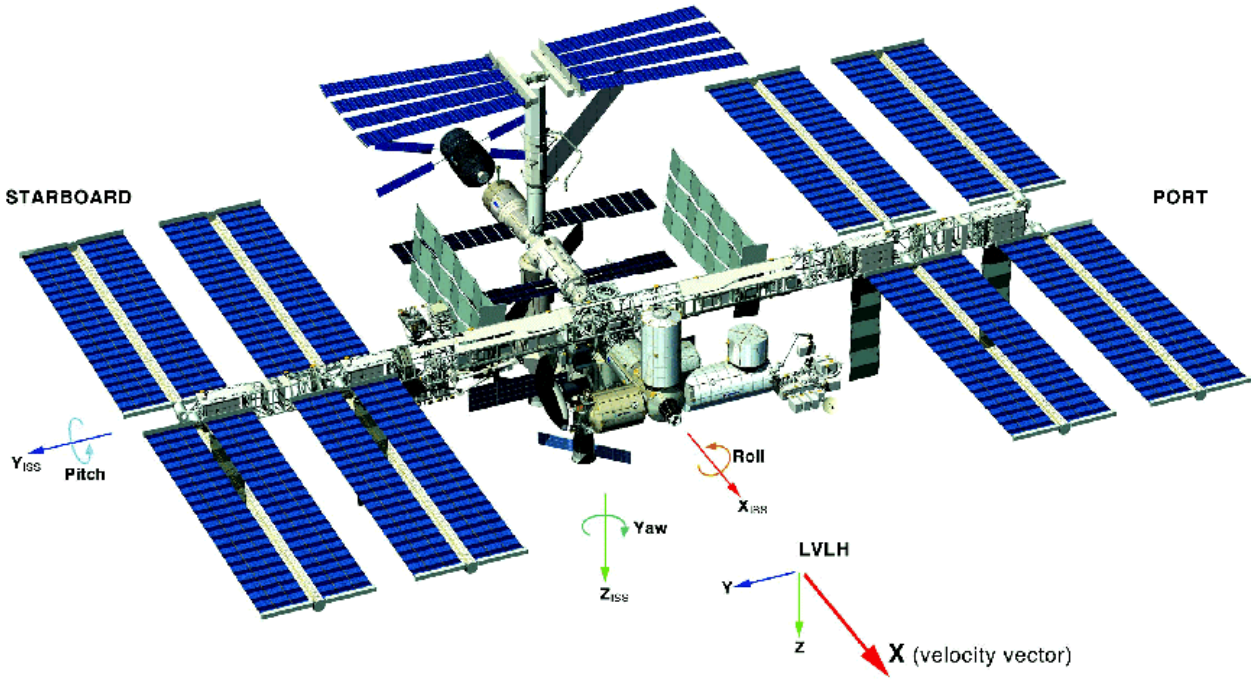

Figure 6-17: The International Space Station (from Carey et al. [2001]).

Table 6-3: Technical parameters of the International Space Station (from Carey et al. [2001]).

PARAMETER	CHARACTERISTIC
Truss length	108 m
Total module length	74 m
Mass	~ 420 tonnes
Maximum power output	110 kW (30 kW for payloads)
Total pressurised volume	1200 m^3
Atmospheric pressure	1013 mbar (1 atmosphere)
Orbital altitude	350 – 460 km
Orbital inclination	51.6°
Orbital velocity	~ 8 km/s
Attitude	Local Vertical Local Horizontal
Maximum crew	7
Data rate uplink	72 kbits/s
Data rate downlink	43 Mbits/s[a]
Ku-band coverage	68% of time
S-band coverage	50% of time
Anticipated lifetime	>10 years

Table 6-4: System parameters of a potential InSAR system on the International Space Station.

Radar Frequency [GHz]	9.7
Polarization	VV
Incidence Angle [deg]	40
Altitude [km]	400
Velocity [m/s]	8000
Eff. No. of Looks[1]	230
Noise Equ. NRCS [dB]	–27.9

[1]) for a 25 m × 25 m resolution cell

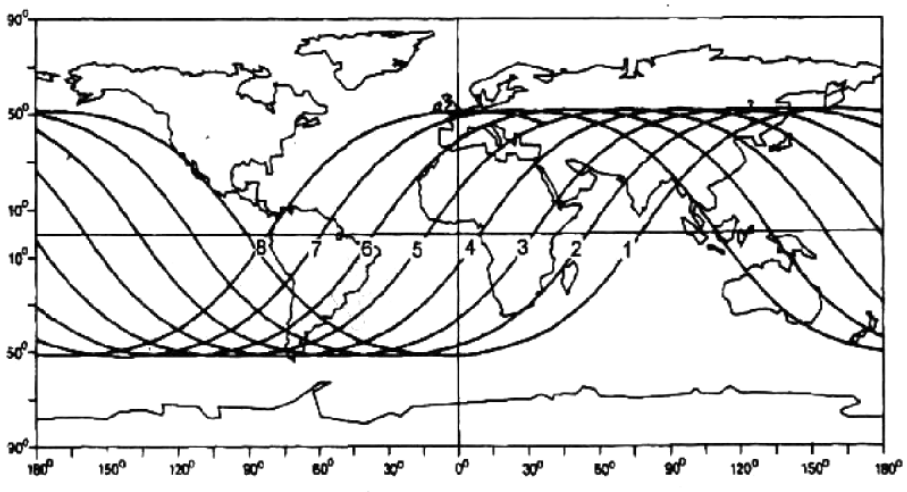

Figure 6-18: Ground track pattern of the International Space Station (from Carey et al. [2001]).

6.4.2. Simulated Data Products

Figure 6-19 shows simulated phase signatures of our test current field. The figure depicts that the proposed InSAR configuration would be capable of detecting current variations smaller than 0.1 m/s on length scales on the order of 100 m. Due to the higher incidence angle, the imaging mechanism would be more linear than in case of a "Interferometric Cartwheel" or "Interferometric Pendulum" with *TerraSAR-X*, but, on the other hand, the SNR would be worse.

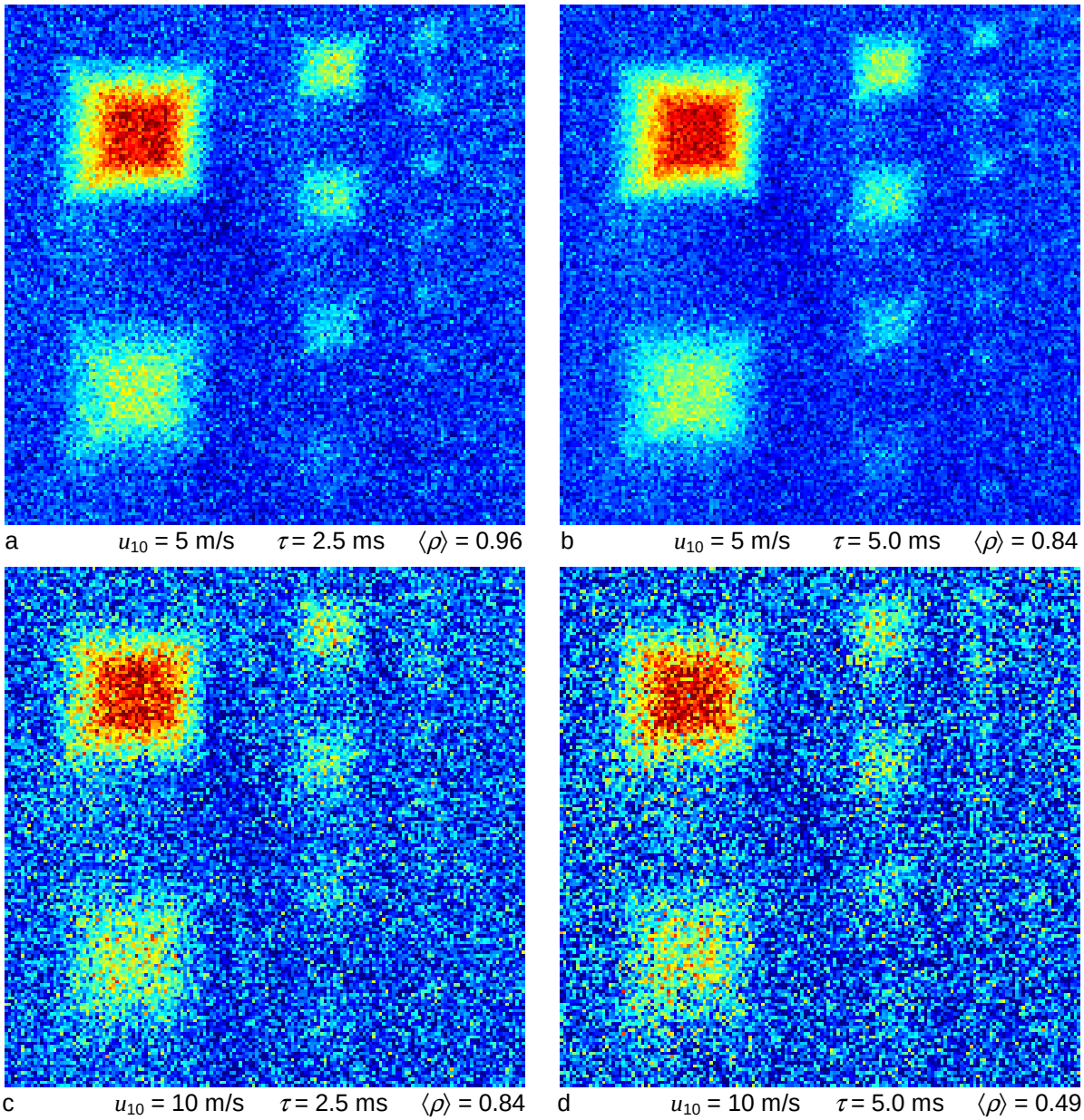

Figure 6-19: Simulated realizations of phase images of the current field of Figure 6-1 as seen by the proposed InSAR on the International Space Station for different wind speeds and time lags: (a) 5 m/s and 2.5 ms, (b) 5 m/s and 5.0 ms, (c) 10 m/s and 2.5 ms, (d) 10 m/s and 5 ms.

6.4.3. Evaluation

In terms of dimensions and orbit parameters, the *ISS* would be well suited for current and wave measurements by along-track InSAR. Also a combined along-track / cross-track InSAR installation for measurements over water and land appears to be feasible. However, some technical issues need to be investigated in more detail for a complete evaluation of the suitability of the *ISS* for InSAR: The most important problems in this context appear to be the following:

- Locations of the two InSAR antennas and other hardware components;
- power consumption;

- data storage and data downlink techniques and capacities;
- interference with other instruments;
- weight and size constraints;
- transport and installation procedures;
- effect of platform motions and vibrations.

We cannot discuss these problems in detail in the framework of this report. However, detailed information on the *ISS* and its capabilities is available from the European Space Agency [*Carey et al.* 2001] and other sources. For example Figure 6-19 shows a spectrum of expected vibrations of the *ISS*.

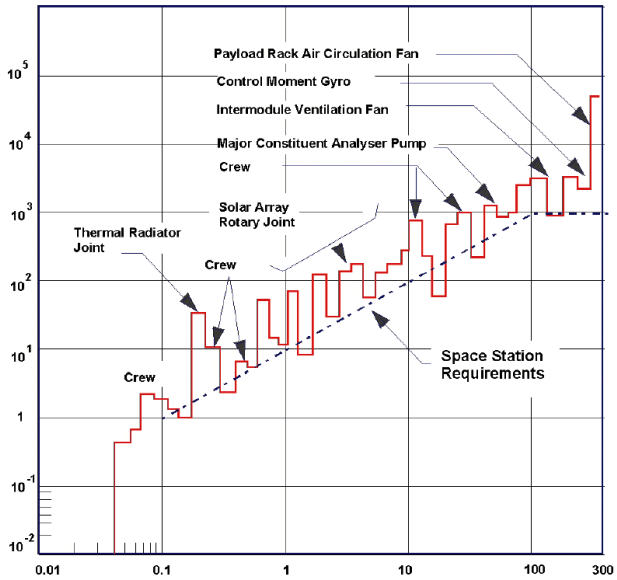

Figure 6-20: Spectrum of vibrations of the International Space Station (from Carey et al. [2001]).

6.5. CONCLUSIONS

In this section we have analyzed the potential of some realistic concepts of spaceborne InSAR systems for oceanic current and wave measurements. We have shown that the most popular concept, the "Interferometric Cartwheel", would be suited for oceanic measurements, but it would not be ideal due to continuously varying along-track baselines which would be too long most of the time. The similar concept of the "Interferometric Pendulum" is clearly preferable from an oceanic applications point of view, since its along-track and cross-track baselines can be individually optimized for current and wave measurements and for measurements over land, and the along-track baselines would be constant. The most promising master satellite for an "Interferometric Cartwheel" or "Interferometric Pendulum" would be *TerraSAR-X*, since it offers the highest spatial resolution and a reasonable SNR. Finally, we have shown that also the *International Space Station* could be an attractive platform for current and wave measurements from space, but there are a number of unresolved technical issues in this context which cannot be discussed in detail in the framework of this report. However, the KoRIOLiS team would be happy to participate in future projects which study the possibilities to install and operate spaceborne InSAR systems on the ISS or other platforms in more detail.

ACKNOWLEDGMENTS

The KoRIOLiS team would like to thank Alberto Moreira from the Institute for High Frequency Technology and Radar Systems, German Aerospace Center, Oberpfaffenhofen, Hartmut Runge from the Remote Sensing Technology Institute, German Aerospace Center, Oberpfaffenhofen, and their co-workers for providing valuable information on the "Interferometric Cartwheel" and the "Interferometric Pendulum", including several figures shown in this section of the KoRIOLiS report, and for a number of fruitful and inspiring discussions and a good collaboration.

REFERENCES

Carey, W., D. Isakeit, M. Heppener, K. Knott, and J. Feustel-Büechl, *The International Space Station European Users Guide*, *ESA Publication UIC-ESA-UM-0001*, available at http://www.spaceflight.esa.int/users/downloads/userguides/ISS_European_Users_Guide.pdf, 2001.

Massonnet, D., Capabilities and limitations of the Interferometric Cartwheel, presented at CEOS SAR Workshop, Toulouse, France, October 1999, available at http://www.estec.esa.nl/CONFANNOUN/99b02/index.html, 1999.

Massonnet, D., E. Thouvenot, S. Ramongassié, and Laurent Phalippou, A wheel of passive radar microsats for upgrading existing SAR projects, in *Proc. 2000 International Geoscience and Remote Sensing Symposium (IGARSS 2000)*, 1000-1003, Inst. of Elec. and Electron. Eng., Piscataway, N.J., USA, 2000.

Mittermayer, J., G. Krieger, M. Wendler, A. Moreira, K.H. Zeller, E. Thouvenot, T. Amiot, and R. Bamler, Preliminary interferometric performance estimation for the Interferometric Cartwheel in combination with ENVISAT ASAR, in *Proc. CEOS 2001*, Tokyo, Japan, 2001a.

Mittermayer, J., G. Krieger, A. Moreira, and M. Wendler, Interferometric performance estimation for the Interferometric Cartwheel in combination with a transmitting SAR satellite, in *Proc. 2001 International Geoscience and Remote Sensing Symposium (IGARSS 2001)*, Inst. of Elec. and Electron. Eng., Piscataway, N.J., USA, 2001b.

Ramongassié, S., L. Phalippou, E. Thouvenot, and D. Massonnet, Preliminary design of the payload for the Interferometric Cartwheel, in *Proc. 2000 International Geoscience and Remote Sensing Symposium (IGARSS 2000)*, 1004-1006, Inst. of Elec. and Electron. Eng., Piscataway, N.J., USA, 2000.

Runge, H., R. Bamler, J. Mittermayer, F. Jochim, D. Massonnet, and E. Thouvenot, The Interferometric Cartwheel for Envisat, in *Proc. 3rd IAA Symposium on Small Satellites for Earth Observation*, Berlin, Germany, April 2001.